ISTITUTO NAZIONALE DI FISICA NUCLEARE

Sezione di Trieste

INFN/TC-92/18

16 luglio 1992

F. Arfelli, G. Barbiellini, P. Bregant, F. Calligaris, G. Cantatore, E. Castelli, L. Dalla Palma, F. de Guarrini, R. Giacomich, R. Longo, A. Penzo, P. Poropat, R. Rosei, M. Sessa, F. Stacul, M. Tonutti, F. Tomasini, G. Tromba, A. Vacchi, R. Vidimari, F. Zanini, C. Zuiani.

SYRMEP (SYnchrotron Radiation for Medical Physics). Performance of the digital detection system

Servizio Documentazione
dei Laboratori Nazionali di Frascati

SYRMEP
(SYnchrotron Radiation for MEdical Physics). Performance of the digital detection system.

F. Arfelli, G. Barbiellini, F. Calligaris, G. Cantatore, E. Castelli, R. Giacomich, A. Penzo, P. Poropat, R. Rosei, M. Sessa, F. Tomasini, A. Vacchi*
Dipartimento di Fisica dell' Università di Trieste
and
Sezione INFN di Trieste

L. Dalla Palma, R. Longo, F. Stacul , M. Tonutti, C. Zuiani
Istituto di Radiologia dell' Università di Trieste
and
USL - Trieste

P. Bregant F. de Guarrini, R. Vidimari
Servizio di Fisica Sanitaria, USL - Trieste

G. Tromba, F. Zanini
Società Sincrotrone Trieste

ABSTRACT

A beamline devoted to mammography has been approved at the synchrotron radiation source Elettra under construction in Trieste, Italy. The SYRMEP program envisions using well-collimated, high intensity, tuneable monochromatic X-ray beams from this source in conjunction with a new digital detection system based on a silicon detector. In this paper we present a status report on this program. In the first part a Monte Carlo simulation illustrates the superior contrast resolution of a monochromatic beam compared to a standard beam from a mammographic tube. In the second part experimental images obtained by means of our new silicon detector are shown. These images clearly show that this feasibility study is giving positive and encouraging results.

*) Società Sincrotrone Trieste.

1. INTRODUCTION

A proposal for a beamline devoted to medical physics has been presented by our collaboration to the Program Advisory Committee (PAC) of the Trieste synchrotron radiation source Elettra in September 1991[1]. As a starting point for this activity, and taking into account the general characteristics of the Elettra facility, we have considered X-ray mammography as a very interesting field of application for synchrotron radiation, particularly suited to the Elettra beam energy.

In the January 1992 meeting, the PAC recommended that a bending magnet port be allocated to the Mammography Program. We, as users, were given the responsibility of beamline and detector development, while experiments on live patients were to be avoided, at least at this early stage. This recommendation has been finally approved by the board of directors of Elettra during the February 1992 meeting. Therefore, at this point, the SYRMEP program is fully operational. Meanwhile the study of the final design of the synchrotron radiation beamline is in progress, and we expect the SR beam to be available by the beginning of 1994.

To find the best working conditions so as to obtain the maximum diagnostic efficiency, while delivering the minimum possible dose to the patient, we intend to take advantage of both the monochromaticity of the synchrotron laminar beam, and of the availability of a new digital detection system.

We have already discussed the effect of the monochromaticity of the laminar beam, showing the signal-to-noise ratio, as a function of the X-ray energy, obtained by a Monte Carlo simulation of the experiment[2]. The basic characteristics of the silicon detector can be found in the paper presented at the 1991 A.I.F.B. annual meeting[3].

In this paper we first discuss the Monte Carlo simulated images of an object illuminated by a standard X-ray mammographic tube and then by a monochromatic beam. This object is assumed to be seen by a 100% efficient detector. Next we show the experimental digital images of a lead mask exposed to an X-ray radioactive source placed in front of our silicon detector. Finally, we discuss the present results pointing out foreseeable future steps.

2. MONTE CARLO SIMULATION

Monte Carlo simulations can be used to evidence the improvements in mammographic image quality which could be achieved using synchrotron radiation (SR) laminar monochromatic X-ray beams, as opposed to conventional X-ray generators. We have performed several simulations with the help of the EGS4[4] code. This program takes into account all the possible interactions of photons with matter: photoelectric effect and Compton and Rayleigh scattering.

We present here results obtained simulating a phantom irradiated by a laminar monochromatic beam and by a non-monochromatic conventional beam. The phantom consists of a 5 cm thick rectangular box containing a 50% mixture of water and fat, which represents the background. The detail to be detected is a 1 cm diameter cylindrical object placed in the centre of the box. To simulate a calcification the object is assigned a thickness of 0.5 mm of Ca, whereas to simulate a nodule we used a 5 mm thickness of water.

First, irradiation by a SR laminar beam has been simulated, where the complete image was obtained by scanning the phantom with a monochromatic X-ray beam having a rectangular section of 10×0.1 cm^2. The active area of the detector was assumed to cover the entire section of the beam transmitted through the phantom. Detection efficiency was assumed to be 100%. In the second case, the Monte Carlo code has been run substituting the SR source with a non-monochromatic conventional beam having a section of 10×10 cm^2 and the typical energy spectrum of an X-ray tube[5]. Table I summarises the results.

Table I (see text)

Beam	*Energy (spectrum)*	*Detail*	*SNR**	*Sup.Dose (μGy)*	*Dose@2cm (μGy)*
Large	30 kV[6] (tube spect.)	Calcific.	20.5	9.9	2.2
Large	30 kV[6] (tube spect.)	Nodule	2.1	9.9	2.2
Laminar	22.5 keV (monochr.)	Calcific.	35.6	4.9	2.9
Laminar	20 keV (monochr.)	Nodule	5.6	6.2	2.9

*SNR is the signal-to -noise ratio[2]

We have assumed comparable doses absorbed at the depth of 2 cm corresponding to the same incident fluence and to the superficial doses given in Table I.

The typical superficial dose absorbed during a mammographic examination can reach the order of magnitude of a mGy. Unfortunately, the Monte Carlo requires a large amount of computer time, and therefore it was not possible to simulate the dose used in real examinations. The difference in the rendition of a nodule in the two cases is readily perceived when comparing the simulated images shown in Figure 1a) and in Figure 1b), even at doses much lower than the ones used in standard practice. For instance, with a water nodule as the detail, the signal-to-noise ratio (SNR) is 5.6 with a 20 keV laminar

beam, while it is 2.1 with a large non-monochromatic beam, under the same conditions of dose absorption at the depth of 2 cm.

3. EXPERIMENTAL IMAGES - APPARATUS AND RESULTS

1) Experimental set-up

Figure 2 shows the apparatus used to produce digital images of a lead mask with a conventional X-ray point source, a solid-state silicon detector, and its associated electronics. The relevant parts of this apparatus are briefly discussed below.

a) X-ray source - The source of gamma radiation was a variable energy X-ray source (code AMC.2084, Amersham Int. plc, Little Chalfont Amersham, Buck., England) consisting of a primary ^{241}Am source sealed in a ceramic casing. The X-rays from the primary source can strike 6 different user-selectable metal targets, thereby exciting fluorescence radiation of different energies. The Tb target was used to obtain 44.2 keV X-rays with a total yield of 7.6×10^{-4} photons/s·sterad. To irradiate the mask-detector assembly in a reproducible way the source was secured to a suitable holder which could be positioned at different distances from the detector.

b) Mask and detector - The object to be imaged was a 500 μm thick lead mask where two letters had been carved out to allow the transmission of photons. Letter width was about 1 mm. Total mask area was 25x30 mm^2. The mask could be moved in front of the detector by means of a micrometer movement stage.

The detector proper was a solid-state silicon strip detector made by Hamamatsu Photonics K.K., Japan. A detailed description of this device can be found in reference [3]. In our application the radiation was impinging on the side of the Si chip rather that on one of its larger surfaces. This choice of geometry has two main consequences. First of all, the detection efficiency is greatly increased, since X-rays will have to traverse a depth of 30 mm of silicon rather than a thickness of 500 μm. For 40 keV X-rays the mass attenuation coefficient is 7.01×10^{-1} cm^2/g: with a Si density of 2.328 g/cm^3 this means that one can expect practically all photons to be absorbed, as opposed to only 7.8% absorption in 500 μm. Detection efficiency is of paramount importance in medical applications since with increased efficiency the radiation dose delivered to the patient can be correspondingly reduced. As a second consequence one has that the spatial resolution in two dimensions of the detector is now determined by strip width and chip thickness, without the need for a second array of microstrips to be deposited at right angles to the first one. Thus, for our imaging purposes, in the following we will speak of detector pixels, each one having a sensitive surface of 500×500 μm^2.

The above geometry, on the other hand, also presents a drawback, namely the fact that, due to fabrication reasons, there is a dead layer of about 700 μm of Si on the detector side, before the microstrips. This dead layer, however, only absorbs about 11% of the incident 40 keV photons, and therefore it does not significantly degrade detection efficiency. Moreover, using newer detector designs, this layer could be reduced to 150 μm, which will absorb only about 2.5% of the photons.

c) Electronics - The charge collected at a microstrip was converted to a voltage signal, with amplitude proportional to the total charge, by means of a charge-sensitive preamplifier. Care was exercised in mounting the preamplifier inputs as close as possible to the corresponding microstrip in order to minimise noise caused by stray capacitance. The signal output by a channel of the preamplifier was further amplified by a fast amplifier (mod. 612A, LeCroy corp., Chestnut Ridge, NY, U.S.A.) and fed to a discriminating circuit (mod. 623B, LeCroy corp., Chestnut Ridge, NY, U.S.A.). The discriminator provided standard negative NIM signals which were counted by a CAMAC scaler (mod. 2551/W, LeCroy corp., Chestnut Ridge, NY, U.S.A.). Data from the scaler were read and stored by means of an Apple Macintosh IIsx computer. In total, 15 microstrips were equipped with the above electronic counting chain. This corresponds to 15 detector pixels, for a total sensitive area of 7.5×0.5 mm^2.

2) Results

Images were produced in the following way. The mask, mounted on a manual micrometer movement stage was placed as close as possible, typically a few mm, to the detector sensitive surface. The source was then positioned at different distances from the detector, typically 4 cm to 8 cm, and centred on the sensitive surface. Preliminary measurements included a background run, done with a 500 μm thick lead screen in front of the detector, and a maximum intensity run, with no screen in front of the detector. An imaging scan consisted of accumulating counts for a set amount of time, manually moving the movement stage by 500 μm, and restarting data acquisition, typically 40 times for each image. In this case the imaged surface would be 7.5×20 mm^2. Considering the fact that, with the photon yield given above, the flux per pixel was only 9.4 photons/s at 4 cm and 2.6 photons/s at 8 cm, counting time was set to 60 s, with the double aim of obtaining meaningful counting statistics and a reasonable total measuring time.

Data were stored in the form of a matrix with 15 rows and 30 columns. From each column of the raw data matrix, background counts from the background run were subtracted. Then, after normalisation to the counts of the maximum intensity run, a scale of grey was assigned to each matrix cell. Figures 3a)-c) show two images thus obtained and the mask used to produce them. Figure 3a) and Figure 3b) show images

obtained placing the source at a distance of 4 cm and 8 cm from the mask, respectively. The mask itself is shown in Figure 3c). Note that the image taken with the source at 8 cm is in a somewhat sharper focus than the other one. This of course should be the case.

To further illustrate the diagnostic value of the digital images which can be obtained with our detector, we fed the raw data from one of the imaging runs into a commercial medical imaging machine. Figure 4a) shows the digital image of the lead mask described above as it resulted when transposed on conventional radiographic film. Figure 4b) shows the same image where the data have been smoothed.

4. DISCUSSION

We present here for the first time digital images obtained with a silicon detector similar to the one already proposed in recent works. This not only proves the feasibility of the detection scheme itself, but also shows how it is possible to achieve a meaningful imaging capability while delivering to the sample a much lower radiation dose than the one necessary when using conventional film as the detector.

We will, therefore, improve the silicon detector by increasing the number of active channels (pixels) in such a way as to cover a larger sensitive area. We also plan to use as a source a conventional mammographic X-ray tube, first as is, and subsequently trying to achieve, by means of suitable filtration techniques, some degree of monochromaticity. This will enable us to produce images of more meaningful objects, standard phantoms for instance, from a medical imaging point of view, using both our detector, and, as a comparison, a conventional film.

Figure captions

Fig. 1- a) Monte Carlo image of a phantom, consisting of a 50% water and fat mixture, with a 1 cm diameter, 5 mm thick, water detail at its centre, irradiated by a large area 30 kV[6] conventional X-ray beam. b) Monte Carlo image of the same phantom as in Figure 1a) irradiated by a laminar, monochromatic, SR X-ray beam.

Fig. 2) - Experimental set-up (see text).

Fig. 3 - a) Digital image of a lead mask (see text). Source to detector distance is 4 cm. b) Same as in Figure 3a) with 8 cm source to detector distance. c) Lead mask (see text).

Fig. 4 - a) Conventional radiographic film rendition of the same image as in Figure 3b) (see text). b) Same as in Figure 4a) with data smoothing.

References and notes

[1] SYRMEP proposal, Sincrotrone Trieste internal report (1991).

[2] L. Benini et al., "Synchrotron Radiation Application to Digital Mammography. A Proposal for the Trieste project 'Elettra'", Phys. Med., Vol. VI, N. 3-4 (1990), p. 293-298.

[3] G. Barbiellini et al., "Solid state detectors for X-rays from Synchrotron Radiation", VI Congresso Nazionale A.I.F.B., Genova, Italy (1991), in press.

[4] W.R. Nelson, H. Hirayama, D.W.O. Rogers, "The EGS4 code system", Stanford Linear Accelerator Center report n. SLAC-265, (1985).

[5] Typical X-ray spectra, for different potentials, can be found in: The Hospital Physicists' Association, "Catalogue of Spectral Data for Diagnostic X-rays", Harwell, U.K., (1979).

[6] The 30 kV figure refers to the potential applied to a commercial, Mo anode, mammographic tube.

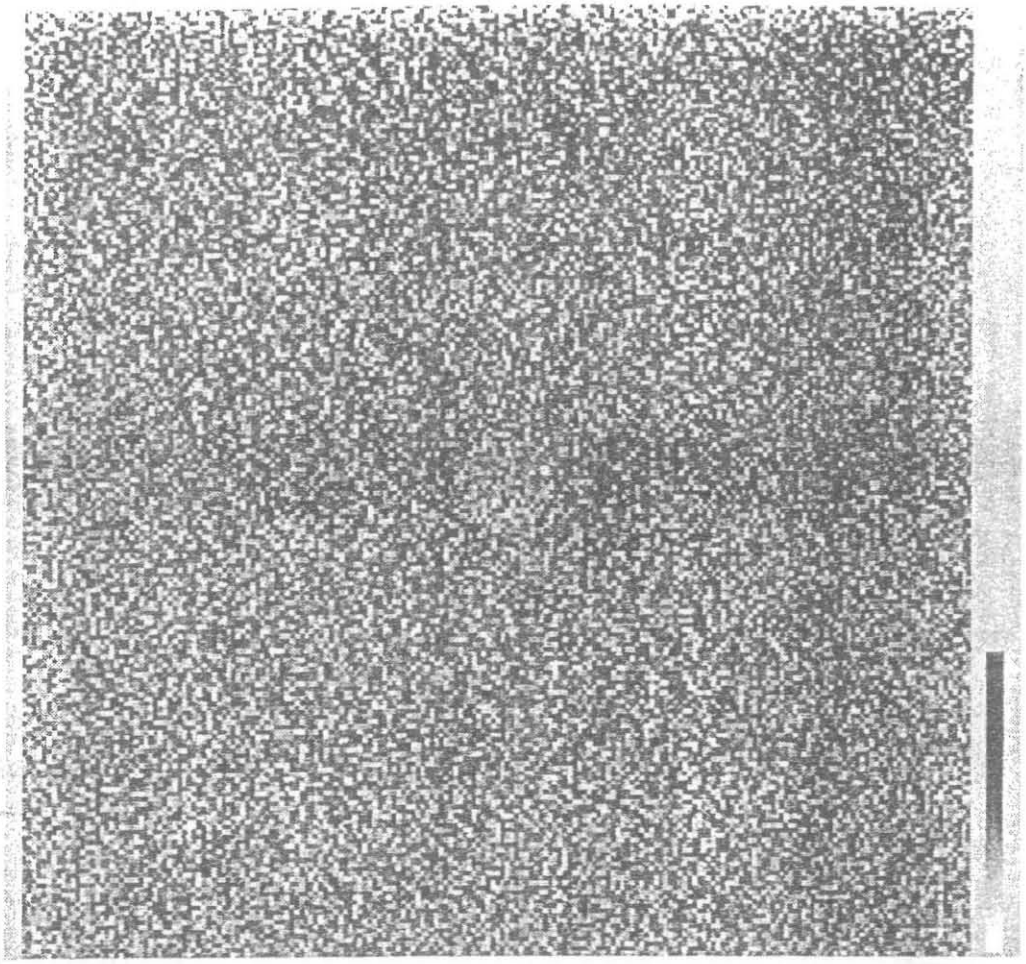

Fig. 1a

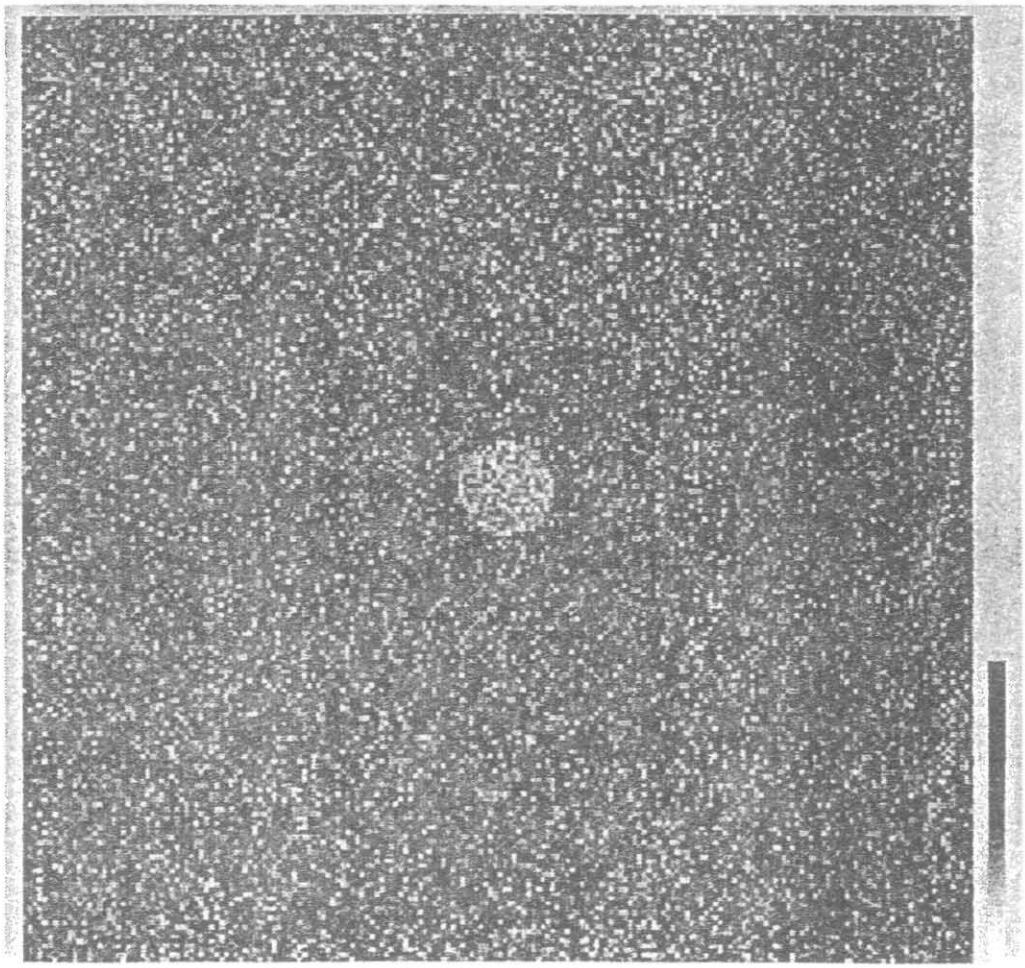

Fig. 1b

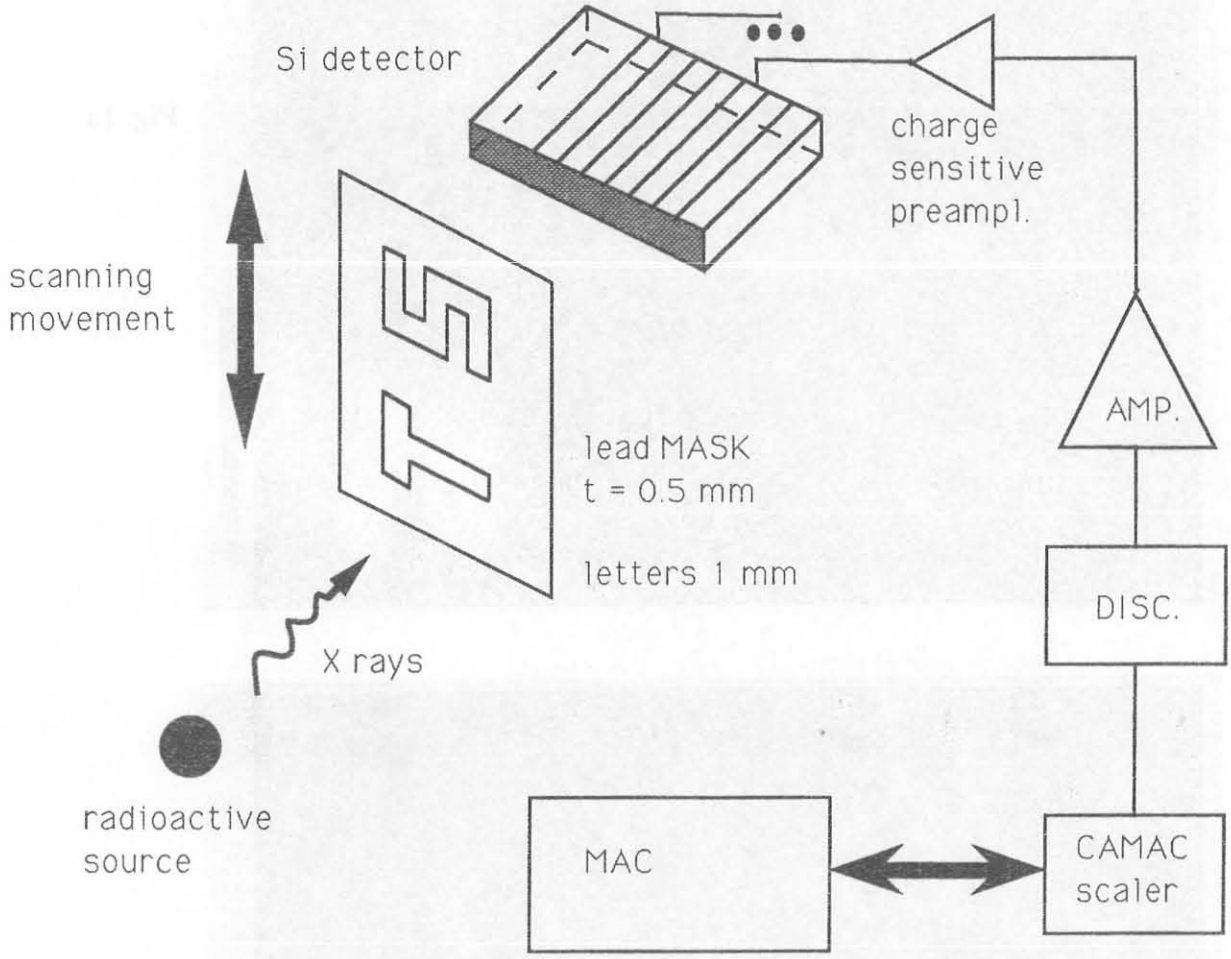
Si detector
charge
sensitive
preampl.
scanning
movement
AMP.
lead MASK
t = 0.5 mm
letters 1 mm
DISC.
X rays
radioactive
source
MAC
CAMAC
scaler

Fig. 2

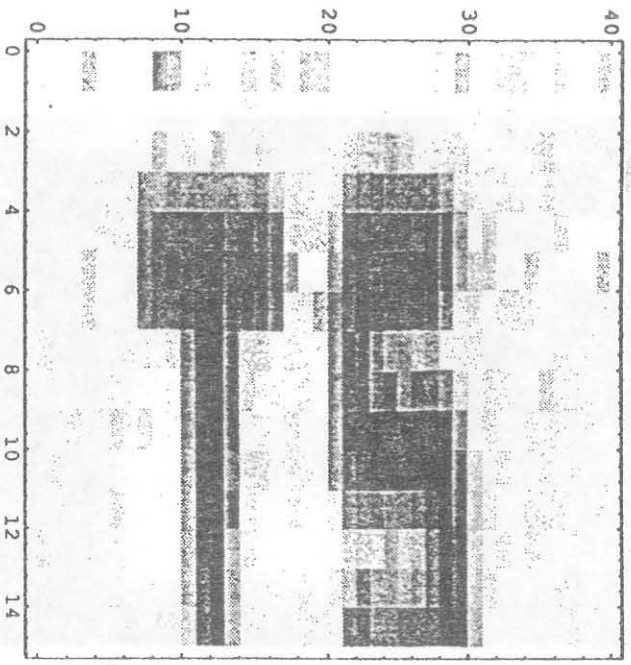

Fig. 3 a

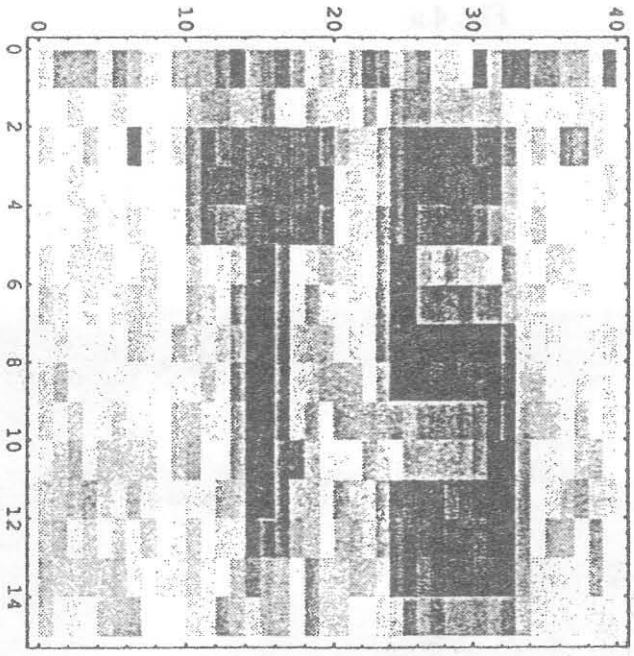

Fig. 3 b

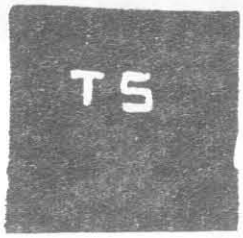

Fig. 3 c

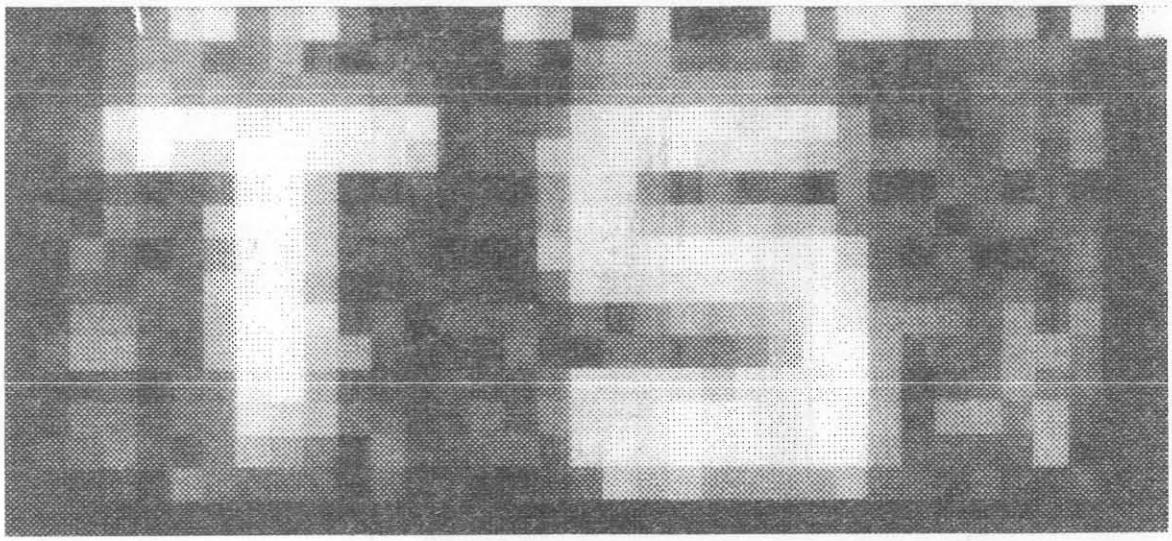

Fig. 4 a

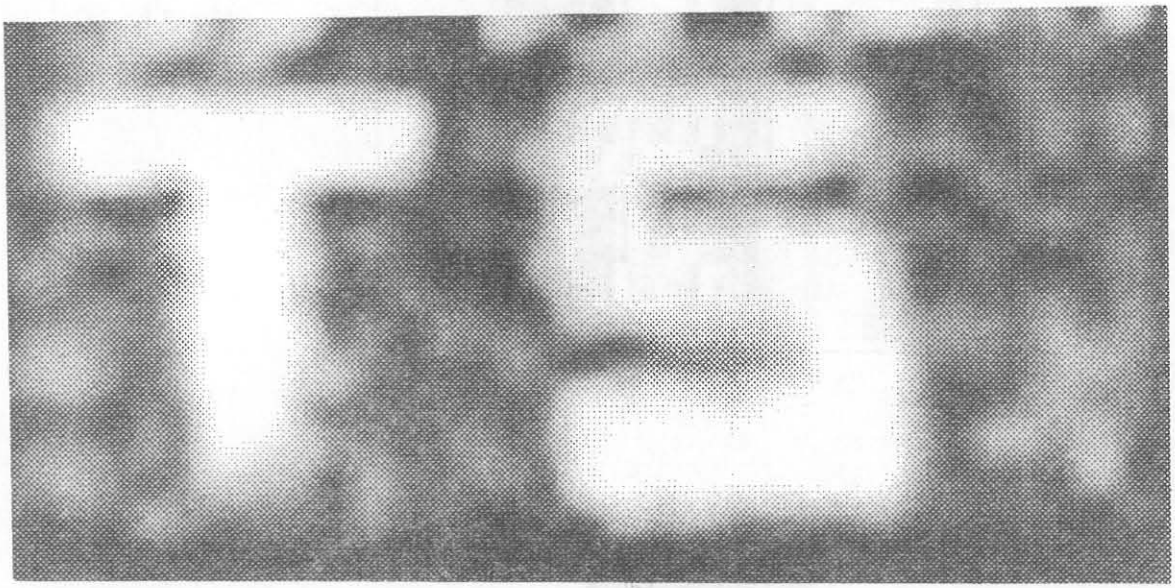

Fig. 4 b